Inorg. Chem. **2003**, *42*, 8309–8319

Solvent Effects on the Electrochemistry and Spectroelectrochemistry of Diruthenium Complexes. Studies of $Ru_2(L)_4Cl$ Where L = 2-CH_3ap, 2-Fap, and 2,4,6-F_3ap, and ap Is the 2-Anilinopyridinate Anion

Karl M. Kadish,*,† Li-Lun Wang,† Antoine Thuriere,† Lingamallu Giribabu,† Rachel Garcia,†,‡ Eric Van Caemelbecke,†,‡ and John L. Bear*,†

Departments of Chemistry, University of Houston, Texas 77204-5003, and Houston Baptist University, 7502 Fondren Road, Houston, Texas 77074-3298

Received June 24, 2003

Three Ru_2^{5+} diruthenium complexes, (4,0) $Ru_2(2\text{-}CH_3ap)_4Cl$, (3,1) $Ru_2(2\text{-}Fap)_4Cl$, and (3,1) $Ru_2(2,4,6\text{-}F_3ap)_4Cl$ where ap is the 2-anilinopyridinate anion, were examined as to their electrochemical and spectroelectrochemical properties in five different nonaqueous solvents (CH_2Cl_2, THF, PhCN, DMF, and DMSO). Each compound undergoes a single one-electron metal-centered oxidation in THF, DMF, and DMSO and two one-electron metal-centered oxidations in CH_2Cl_2 and PhCN. The three diruthenium complexes also undergo two reductions in each solvent except for CH_2Cl_2, and these electrode processes are assigned as $Ru_2^{5+/4+}$ and $Ru_2^{4+/3+}$. Each neutral, singly reduced, and singly oxidized species was characterized by UV–vis thin-layer spectroelectrochemistry, and the data are discussed in terms of the most probable electronic configuration of the compound in solution. The three neutral complexes contain three unpaired electrons as indicated by magnetic susceptibility measurements using the Evans method (3.91–3.95 μ_B), and the electronic configuration is assigned as $\sigma^2\pi^4\delta^2\pi^{*2}\delta$, independent of the solvent. The three singly oxidized compounds have two unpaired electrons in CD_2Cl_2, DMSO-d_6, or CD_3CN (2.65–3.03 μ_B), and the electronic configuration is here assigned as $\sigma^2\pi^4\delta^2\pi^{*2}$. The singly reduced compound also has two unpaired electrons (2.70–2.80 μ_B) in all three solvents, consistent with the electronic configuration $\sigma^2\pi^4\delta^2\pi^{*2}\delta^{*2}$ or $\sigma^2\pi^4\delta^2\pi^{*3}\delta^*$. Finally, the overall effect of solvent on the number of observed redox processes is discussed in terms of solvent binding, and several formation constants were calculated.

We recently reported the electrochemistry, spectroelectrochemistry, and structural properties of a series of $Ru_2(L)_4Cl$ complexes where L = 2-CH_3ap, 2-Fap, 2,5-F_2ap, 2,6-F_2ap, 2,4,6-F_3ap, or F_5ap and ap is the 2-anilinopyridinate anion.[1] The electrochemistry was carried out in CH_2Cl_2 and showed the existence of three well-defined dimetal-centered redox processes as shown by eqs 1−3.

$$Ru_2^{5+} + e^- \rightleftharpoons Ru_2^{4+} \quad (1)$$

$$Ru_2^{5+} \rightleftharpoons Ru_2^{6+} + e^- \quad (2)$$

$$Ru_2^{6+} \rightleftharpoons Ru_2^{7+} + e^- \quad (3)$$

Earlier electrochemical studies on $Ru_2(dpf)_4(CO)$ where dpf is the diphenylformamidinate anion had shown that Ru_2^{3+} and Ru_2^{2+} oxidation states of the dimetal unit could also be electrochemically accessed under a carbon monoxide atmosphere (where one or two CO ligands were axially coordinated),[2] and it was of interest to see if low oxidation state diruthenium complexes might also be obtained for the substituted ap compounds upon coordination of axial ligands other than CO and specifically upon coordination of solvent molecules when the electrochemical measurements were carried out in a bonding solvent.

This is investigated in the present paper for three of the seven previously characterized $Ru_2(L)_4Cl$ derivatives, whose electrochemistry was only known in the noncoordinating solvent CH_2Cl_2.[1] The investigated compounds are (4,0) $Ru_2(2\text{-}CH_3ap)_4Cl$, (3,1) $Ru_2(2\text{-}Fap)_4Cl$, and (3,1) $Ru_2(2,4,6\text{-}F_3ap)_4Cl$ (see Chart 1) while the investigated solvents are

* To whom correspondence should be addressed. E-mail: kkadish@uh.edu (K.M.K.).
† University of Houston.
‡ Houston Baptist University.

(1) Kadish, K. M.; Wang, L.-L.; Thuriere, A.; Van Caemelbecke, E.; Bear, J. L. *Inorg. Chem.* **2003**, *42*, 834.
(2) Kadish, K. M.; Boacheng, H.; Shao, J.; Ou, Z.; Bear, J. L. *Inorg. Chem.* **2001**, *40*, 6848.

10.1021/ic034722d CCC: $25.00
Published on Web 11/01/2003

Chart 1. Schematic Representation of the Three Compounds Investigated in This Work

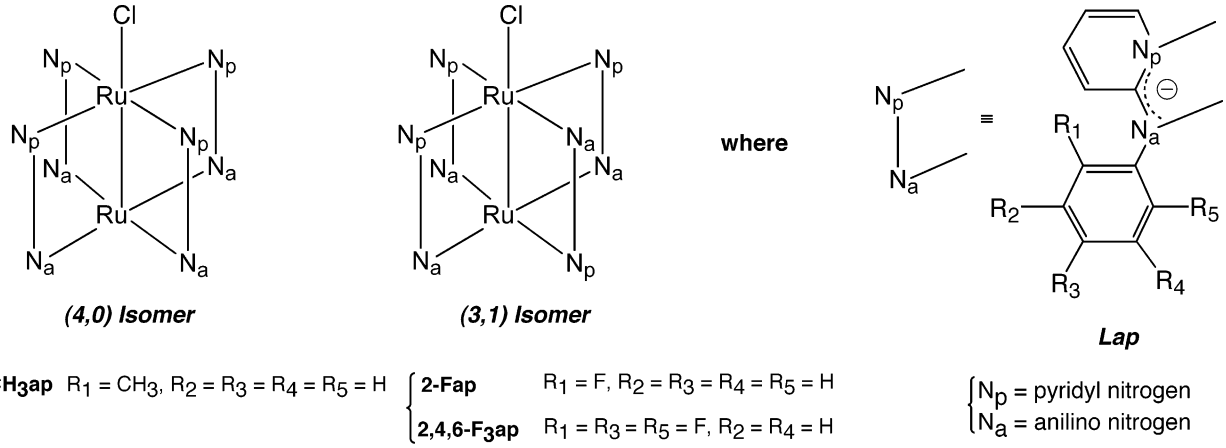

Table 1. Abbreviations and Parameters of Solvents Investigated[a]

abbrev	solvent	ϵ	E_T	ACN	DN
THF	tetrahydrofuran	7.6	0.207	8.0	20.0
CH_2Cl_2	dichloromethane	8.9	0.309	20.4	0.0
PhCN	benzonitrile	25.2	0.333	15.5	11.9
DMF	*N*,*N*-dimethylformamide	36.7	0.404	16.0	26.6
DMSO	dimethyl sulfoxide	46.4	0.444	19.3	29.8

[a] ϵ = dielectric constant; E_T = Dimroth−Reichardt parameter at 30 °C; ACN = Gutmann acceptor number; DN = Gutmann donor number.

CH_2Cl_2, THF, PhCN, DMF, and DMSO whose solvent parameters[3−7] (ϵ, E_T, ACN, and DN) are summarized in Table 1.

As part of our study, we were also interested in determining the number of solvent molecules that would coordinate to the neutral, reduced, or oxidized form of each compound, and at the same time, we wished to characterize the UV−vis spectrum of each Ru_2^{n+} derivative (n = 6, 5, or 4) under different solution conditions. This is also investigated in the present paper which utilizes the UV−vis data combined with magnetic susceptibility data of the neutral, singly oxidized, and singly reduced compounds in three solvent to assign the most likely electronic configuration of the compounds actually in solution.

Experimental Section

Chemicals and Reagents. Synthesis and characterization of the compounds investigated in this paper has been described in the literature.[1,8] Tetra-*n*-butylammonium perchlorate (TBAP, Fluka Chemical Co.) was twice recrystallized from absolute ethyl alcohol and dried in a vacuum oven at 40 °C for at least a week prior to use. Absolute dimethyl sulfoxide (DMSO) and *N*,*N*-dimethylformamide (DMF) were obtained from Aldrich Chemical Co. and were used as received without further purification. Absolute dichloromethane (CH_2Cl_2) was purchased from Fluka and used as received. Reagent grade tetrahydrofuran (THF) was first distilled from calcium hydride (CaH_2) and dried over sodium metal pieces and benzophenone. The solvent was refluxed (but not distilled) until the blue color of the benzophenone ketyl radical anion persisted. Benzonitrile (PhCN) obtained from Aldrich Chemical Co. was distilled over phosphorus pentoxide (P_2O_5) under vacuum prior to use.

Instrumentation. Cyclic voltammetry (CV) measurements were carried out with an EG&G model 173 potentiostat. A three-electrode system was used for CV measurements in organic solvents and consisted of a glassy carbon working electrode, a platinum wire counter electrode, and a saturated calomel reference electrode (SCE). The reference electrode was separated from the bulk solution by a fritted-glass bridge filled with the solvent/supporting electrolyte mixture. Solutions containing the diruthenium complexes were deoxygenated by a stream of high purity nitrogen for at least 5 min prior to making electrochemical measurements, and the solutions in the electrochemical cell were protected from air by a blanket of nitrogen during the experiment. All potentials were measured versus the SCE and are reported both versus SCE and versus the ferrocene/ferrocenium (Fc/Fc^+) couple which was used as internal standard.

Spectroelectrochemical experiments were performed using an EG&G model 163 potentiostat and a thin-layer cell whose design has been described in the literature.[9] Time-dependent UV−vis spectra were recorded on a Hewlett-Packard model 8452A diode array spectrophotometer.

Controlled-potential electrolyses to electrogenerate the singly reduced and singly oxidized forms of the compounds were carried out with an EG&G model 173 potentiostat using an "H" type cell which consisted of two cylindrically shaped platinum gauze electrodes as working and counter electrodes separated by a fine fritted disk.

In a typical experiment, 8 mg of the diruthenium complex was dissolved in 5 mL of the deuterated solvent, and after electrolysis at the desired potential, 1 mL of solution was transferred to an NMR tube for magnetic moment measurements using the Evans method. CD_3CN was used instead of PhCN-d_5 due to the significant price difference between the two solvents.

Results and Discussion

Cyclic Voltammetry. Figure 1 illustrates cyclic voltammograms of $Ru_2(2\text{-}CH_3ap)_4Cl$, $Ru_2(2\text{-}Fap)_4Cl$, and $Ru_2(2,4,6\text{-}F_3ap)_4Cl$ in each investigated solvent containing 0.1 M TBAP

(3) Mayer, U.; Gerger, W.; Gutmann, V. *Monatsh. Chem.* **1975**, *106*, 1235.
(4) Gutmann, V. *The Donor−Acceptor Approach to Molecular Interactions*; Plenum Press: New York, 1978.
(5) Gutmann, V.; Wychera, E. *Inorg. Nucl. Chem. Lett.* **1966**, *2*, 257.
(6) Dimroth, K.; Reichardt, C.; Siepmann, T.; Bohlmann. *Liebigs Ann. Chem.* **1963**, *661*, 1.
(7) Reichardt, C.; Harbusch-Gornert. *Liebigs Ann. Chem.* **1983**, 721.
(8) Bear, J. L.; Wellhoff, J.; Royal, G.; Van Caemelbecke, E.; Eapen, S.; Kadish, K. M. *Inorg. Chem.* **2001**, *40*, 2282.
(9) Lin, X. Q.; Kadish, K. M. *Anal. Chem.* **1985**, *57*, 1489.

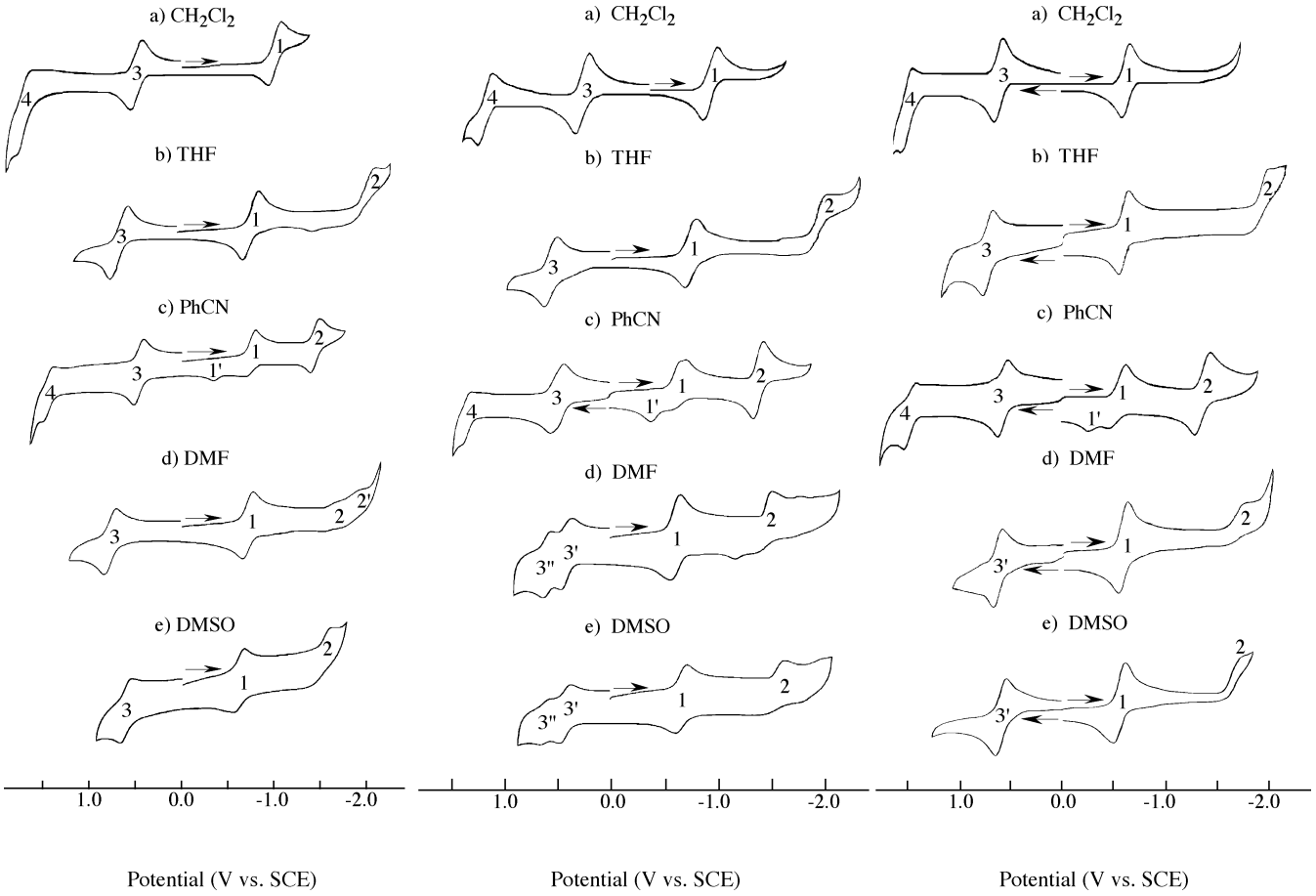

Figure 1. Cyclic voltammograms of $Ru_2(L)_4Cl$ where L = 2-CH_3ap, 2-Fap, or 2,4,6-F_3ap in five investigated solvents containing 0.1 M TBAP as supporting electrolyte. Scan rate = 0.1 V/s. Processes 1 and 2 correspond to reductions and processes 3 and 4 to oxidations.

Table 2. Half-Wave Potentials for Oxidations and Reductions of Ru_2(2-CH_3ap)$_4$Cl, Ru_2(2-Fap)$_4$Cl, and Ru_2(2,4,6-F_3ap)$_4$Cl in Investigated Solvents

	$E_{1/2}$ (V vs Fc/Fc$^+$)[e]				$E_{1/2}$ (V vs SCE)			
solvent	$Ru_2^{7+/6+}$	$Ru_2^{6+/5+}$	$Ru_2^{5+/4+}$	$Ru_2^{4+/3+}$	$Ru_2^{7+/6+}$	$Ru_2^{6+/5+}$	$Ru_2^{5+/4+}$	$Ru_2^{4+/3+}$
				Ru_2(2-CH_3ap)$_4$Cl				
CH_2Cl_2[a]	0.96	−0.07	−1.37		1.44	0.41	−0.89	
THF[b]		0.08	−1.30	−2.62[d]		0.61	−0.77	−2.09[d]
PhCN	0.97	−0.01	−1.23	−1.95	1.45	0.47	−0.75	−1.47
DMF		0.15	−1.09	−1.82/−2.03[c]		0.64	−0.60	−1.33/−1.54[c]
DMSO		0.14	−1.06	−2.04[d]		0.59	−0.61	−1.59[d]
				Ru_2(2-Fap)$_4$Cl				
CH_2Cl_2[a]	0.95	−0.01	−1.25		1.43	0.47	−0.77	
THF[b]		0.05	−1.27	−2.54[d]		0.58	−0.74	−2.01[d]
PhCN	0.86	−0.01	−1.15	−1.91	1.36	0.49	−0.65	−1.41
DMF		−0.09/0.10[c]	−1.11	−1.98/−2.30[c,d]		0.39/0.58[c]	−0.63	−1.50/−1.82[c,d]
DMSO		−0.06/0.12[c]	−1.08	−1.91[d]		0.39/0.57[c]	−0.63	−1.46[d]
				Ru_2(2,4,6-F_3ap)$_4$Cl				
CH_2Cl_2[a]	1.07	0.14	−1.13		1.55	0.62	−0.65	
THF[b]		0.19	−1.12	−2.51[d]		0.72	−0.59	−1.98[d]
PhCN	1.00	0.10	−1.03	−1.86	1.50	0.60	−0.53	−1.36
DMF		0.11	−1.02	−2.11[d]		0.59	−0.54	−1.63[d]
DMSO		0.12	−0.97	−2.10[d]		0.57	−0.52	−1.65[d]

[a] Taken from ref 1. [b] TBAP (0.2 M) was used as the supporting electrolyte. [c] Two processes were observed. [d] E_{pc}. [e] The values of the Fc/Fc$^+$ couple are as follows vs SCE: CH_2Cl_2 (0.48 V), THF (0.53 V), PhCN (0.48 V), DMF (0.49 V), and DMSO (0.45 V). Unless otherwise indicated, all values of $E_{1/2}$ represent reversible reactions.

as supporting electrolyte while a summary of half-wave potentials for each electrode process is given in Table 2 (as measured versus SCE and versus the Fc/Fc$^+$ couple to account for junction potential differences among the solvents).

As has been previously shown,[1] the three investigated compounds undergo two reversible one-electron oxidations and a single reversible one-electron reduction in CH_2Cl_2. These electrode reactions are labeled as processes 1, 3, and 4 in Figure 1. An additional one-electron reduction, labeled

Scheme 1

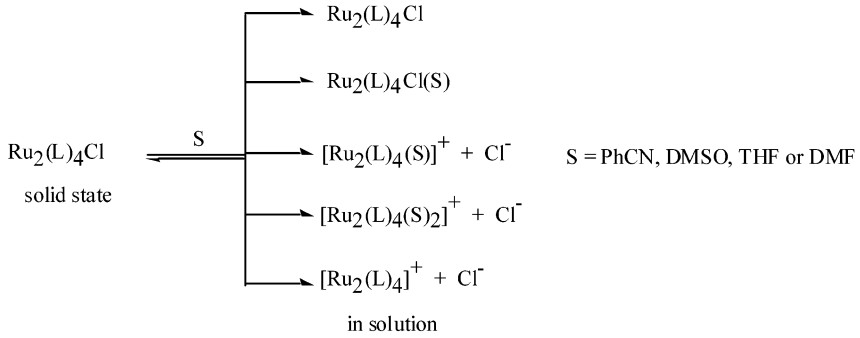

as process 2 in Figure 1, is also observed in all solvents except CH_2Cl_2, and this process is assigned to the $Ru_2^{4+/3+}$ redox couple on the basis of comparisons with similar reactions of $Ru_2(dpf)_4(CO)$ in CH_2Cl_2.[2]

The reversibility, peak current heights, and half-wave or peak potentials for the $Ru_2^{4+/3+}$ processes are in each case a function of the electrochemical solvent (see Table 2 and Figure 1). The reaction is reversible for all three compounds in PhCN (curves c in Figure 1) and occurs at $E_{1/2}$ values which range from −1.36 (L = 2,4,6-F_3ap) to −1.47 V (L = 2-CH_3ap) versus SCE. In contrast, the $Ru_2^{4+/3+}$ process is irreversible in THF and located at cathodic peak potentials of −1.98 V (L = 2,4,6-F_3ap) to −2.09 V (L = 2-CH_3ap) for a scan rate of 0.1 V/s.

An irreversible $Ru_2^{4+/3+}$ process is also observed in DMSO and DMF (see Figure 1), and thus, PhCN is the only one of the five solvents which provides a facile and reversible access to the Ru_2^{3+} oxidation state for the three compounds. At the same time, however, it should be noted that the $Ru_2^{5+/4+}$ process of the three complexes in PhCN is characterized by two reoxidation peaks, and as will be discussed in later sections of the manuscript, this is related to an equilibrium between two different forms of the singly reduced product on the cyclic voltammetry time scale, one of which contains bound Cl^- anion and the other a bound PhCN molecule.

UV−Vis Characterization of Initial Ru_2^{5+} Complexes. Five possible forms of the diruthenium(III,II) complex might be obtained upon dissolving $Ru_2(L)_4Cl$ in a coordinating solvent, and these are illustrated in Scheme 1 where S represents a solvent molecule. Three of the five possible Ru_2^{5+} complexes in solution are shown with a dissociated Cl^- anion and thus carry a single positive charge on the $[Ru_2(L)_4]^+$ unit; the other two possible species are shown as uncharged by virtue of the fact that the Cl^- anion remains coordinated to the $[Ru_2(L)_4]^+$ unit in solution.

The UV−vis spectra of $Ru_2(L)_4Cl$ should depend on the number and type of axial ligands bound to the Ru_2^{5+} complex. Different UV−vis spectra would be expected if the Cl^- remained associated to $Ru_2(L)_4Cl$ (as in CH_2Cl_2) than if it were displaced by a solvent molecule, giving an overall singly charged Ru_2^{5+} species in solution, either $[Ru_2(L)_4(S)]^+$ or $[Ru_2(L)_4(S)_2]^+$ (see Scheme 1). In contrast, only small changes in the UV−vis spectra would be expected in the absence of solvent binding to $Ru_2(L)_4Cl$ or when the solvent were only weakly coordinated trans to Cl^-, i.e., in the case of $Ru_2(L)_4Cl(S)$.

Table 3. Absorption Maxima of Neutral, Reduced, and Oxidized $Ru_2(L)_4Cl$, Where L Is 2-CH_3ap, 2-Fap, or 2,4,6-F_3ap

oxidn state	ligand	solvent	λ_{max}, nm ($\epsilon \times 10^{-3}$, M^{-1} cm^{-1}) band I	band II	band III	band IV
Ru_2^{4+}	2-CH_3ap	CH_2Cl_2		534 (3.6)		729 (0.8)
		THF	450 (5.6)	534 (2.9)		693 (1.1)
		PhCN	460 (6.9)			747 (5.2)
		DMSO	454 (8.7)	533 (6.2)		711 (6.0)
	2-Fap	CH_2Cl_2		482 (s)		
		THF	460 (s)			743 (3.4)
		PhCN	461 (4.3)			750 (2.6)
		DMSO	452 (s)			757 (3.0)
	2,4,6-F_3ap	CH_2Cl_2		476 (s)		
		PhCN	466 (7.6)			761 (2.9)
		DMSO	486 (s)			782 (2.7)
Ru_2^{5+}	2-CH_3ap	CH_2Cl_2	424 (s)	461 (4.7)		764 (7.3)
		THF	420 (s)	463 (4.7)		760 (7.1)
		PhCN	420 (s)	463 (4.9)		764 (7.5)
		DMSO	424 (s)	461 (4.4)		764 (6.7)
	2-Fap	CH_2Cl_2	428 (3.6)	463 (3.6)		750 (3.9)
		THF	426 (4.6)	467 (4.8)		750 (5.0)
		PhCN	436 (3.1)	457 (3.2)		757 (3.7)
		DMSO	434 (s)	459 (3.6)		757 (4.4)
	2,4,6-F_3ap	CH_2Cl_2	418 (4.5)	476 (4.7)		777 (4.5)
		PhCN	422 (4.8)	487 (5.2)		769 (5.3)
		DMSO	414 (3.9)	486 (4.1)		777 (4.3)
Ru_2^{6+}	2-CH_3ap	CH_2Cl_2	443 (6.9)	530 (6.5)		990 (15.9)
		THF	443 (4.9)	529 (4.4)		975 (12.0)
		PhCN	443 (5.4)	532 (4.6)		1000 (11.6)
		DMSO	443 (7.6)	536 (6.8)		991 (10.8)
	2-Fap	CH_2Cl_2	431 (4.1)			960 (5.2)
		THF	432 (4.6)	518 (4.9)		975 (8.3)
		PhCN	423 (2.9)	499 (2.7)	694 (s)	924 (6.7)
		DMSO	430 (5.8)	483 (5.3)		780 (6.1)
	2,4,6-F_3ap	CH_2Cl_2		487 (5.7)	670 (4.4)	965 (9.5)
		PhCN	425 (6.2)	490 (5.6)	690 (3.3)	931 (11.1)
		DMSO	425 (4.0)	487 (4.0)		897 (5.5)

The UV−vis data for each $Ru_2(L)_4Cl$ derivative in the different nonaqueous solvents are summarized in Table 3 which is arranged according to the oxidation state of the dimetal core, i.e., Ru_2^{4+}, Ru_2^{5+}, and Ru_2^{6+}, while examples of spectra for the Ru_2^{5+} species are shown in Figure 2 over the spectral region 400−1000 nm. As seen in the figure, spectral differences exist between the compounds with different bridging ligands (2-CH_3ap, 2-Fap, and 2,4,6-F_3ap), but for each individual derivative, the shape of the overall spectrum and the position of the three major absorption bands are only slightly affected by changes in solvent, with the smallest changes being observed in the case of the 2-CH_3ap

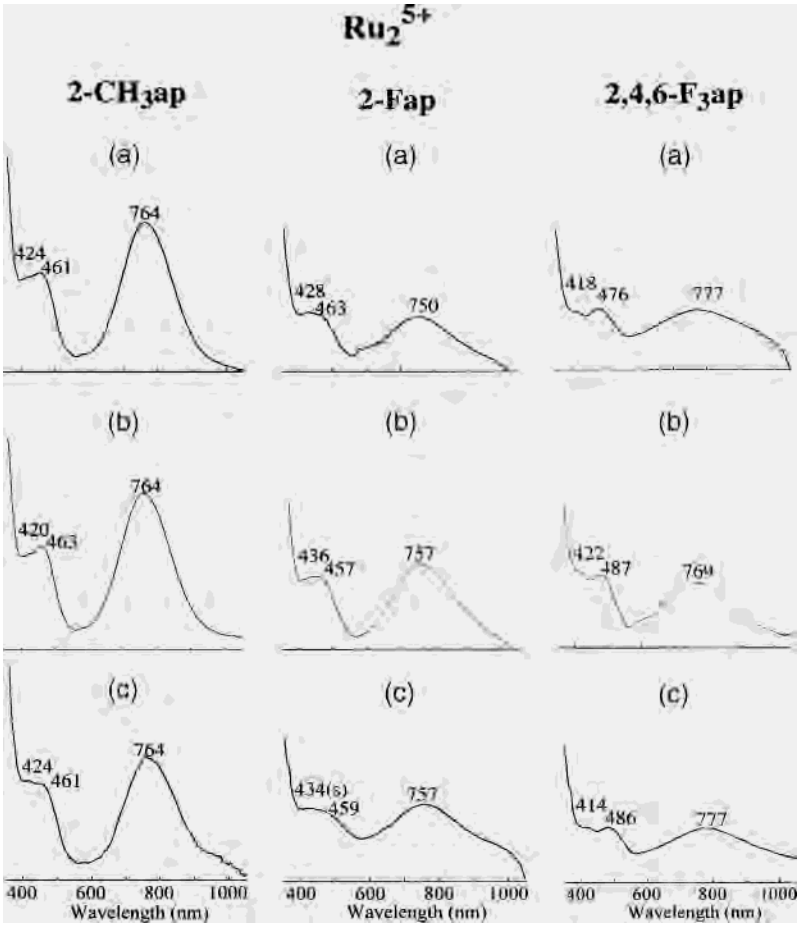

Figure 2. UV−vis spectra (400−1000 nm) (with arbitrary absorbance scale) showing the Ru_2^{5+} forms of each investigated compound in (a) CH_2Cl_2, (b) PhCN, and (c) DMSO containing 0.2 M TBAP.

complex. The results clearly suggest that the Cl^- anion of $Ru_2(2\text{-}CH_3ap)_4Cl$ is not displaced by a THF, PhCN, or DMSO molecule, and a similar conclusion can be drawn in the case of the other two derivatives.

UV−Vis Characterization of Electrogenerated Ru_2^{4+}. The addition of one electron to $Ru_2(L)_4Cl$ might lead to a number of possible Ru_2^{4+} reduction products which can be formulated as $[Ru_2(L)_4Cl]^-$, $Ru_2(L)_4$, $Ru_2(L)_4(S)$, or $Ru_2(L)_4(S)_2$ depending upon the nature of the solvent. The reduced form will in each case have a Ru_2^{4+} core but can differ in the number and/or type of axial ligands bound to the Ru_2^{4+} unit. This point was examined in the current study by thin-layer UV−vis spectroscopic characterization of the first reduction product in each solvent. Examples of the spectral changes which occur upon the first reduction are illustrated in Figure 3 for the case of $Ru_2(2\text{-Fap})_4Cl$ in PhCN (top) and $Ru_2(2\text{-}CH_3ap)_4Cl$ in THF (bottom), both of which contain 0.2 M TBAP. As shown in this figure, the Ru_2^{5+} band at 757 (PhCN) or 760 (THF) nm decreases in intensity and shifts to 750 nm (2-Fap in PhCN) or 693 nm (2-CH_3ap in THF) upon addition of one electron while, at the same time, new bands grow in at 461 nm (2-Fap in PhCN) or 450 and 534 nm (2-CH_3ap in THF). Both sets of spectral changes in Figure 3 are associated with well-defined isosbestic points, thus indicating the absence of any spectral intermediates during the time scale of the experiment.

Similar spectroelectrochemical experiments were carried out for each of the three compounds in the different solvents, and spectral data for the electrogenerated Ru_2^{4+} species under each solution condition are summarized in Table 3. A comparison of the UV−vis spectrum for singly reduced $Ru_2(2\text{-}CH_3ap)_4Cl$ in CH_2Cl_2, THF, PhCN, and DMSO is also illustrated in Figure 4. As shown in this figure, the electrogenerated Ru_2^{4+} complex exhibits similar but not identical spectral features in each solvent. For example, a small but well-defined band is seen at 533−534 nm in CH_2Cl_2, THF, and DMSO, but this band is not present in PhCN. A band at 450−460 nm is seen in THF, PhCN, and DMSO but not in CH_2Cl_2. A broad band is also seen at 693−747 nm in each of the four solvents, and the intensity of this band decreases in the following order: PhCN > DMSO > THF > CH_2Cl_2

The data in Figure 4 suggest a different degree of solvent coordination in CH_2Cl_2 as compared to the other three solvents, but before addressing the form of the Ru_2^{4+} species in coordinating media, it was necessary to examine the fate of the bound Cl^- ion after electroreduction in the noncoordinating solvent, CH_2Cl_2. The reduction of $Ru_2(L)_4Cl$ by one electron in CH_2Cl_2 should lead first to $[Ru_2^{4+}(L)_4Cl]^-$ and then to $Ru_2^{4+}(L)_4$, and one or both reduction products might be observed on the time scale of the electrochemical experiment as is the case for the reduction of these diruthe-

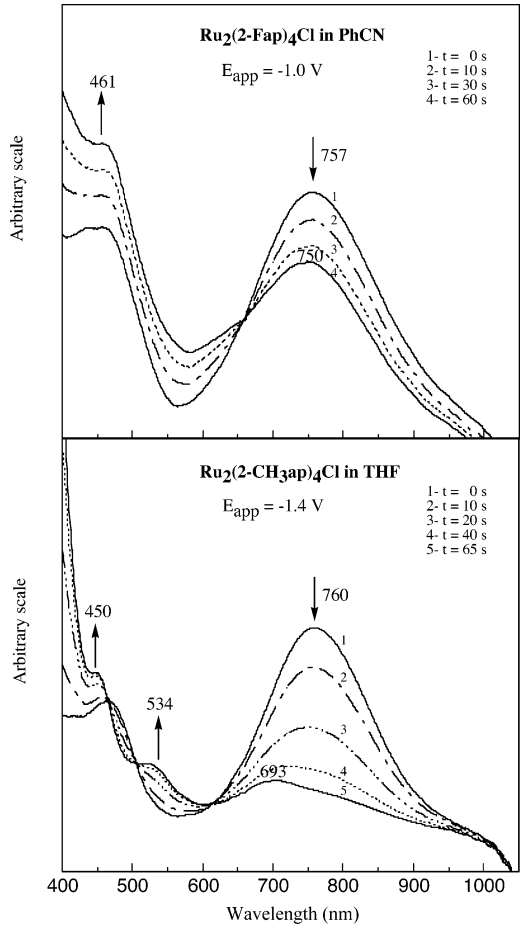

Figure 3. Thin-layer time-dependent UV−vis spectral changes during the $Ru_2^{5+/4+}$ process of (a) $Ru_2(2\text{-Fap})_4Cl$ in PhCN, 0.2 M TBAP, and (b) $Ru_2(2\text{-}CH_3ap)_4Cl$ in THF, 0.2 M TBAP.

nium complexes in CH_2Cl_2[10,11] where the Cl^- is only slowly dissociated after formation of Ru_2^{4+}.

In order to ascertain the fate of the bound Cl^- after electroreduction, spectroelectrochemical experiments were carried out for $Ru_2(2\text{-}CH_3ap)_4Cl$ in CH_2Cl_2 with and without excess Cl^- in solution. The resulting data are shown in Figure 5 which illustrates the initial and final spectra in CH_2Cl_2 containing 0.2 M TBAP with and without added Cl^- in the form of TBACl. As seen in this figure, the same Ru_2^{5+} spectrum is obtained with and without added Cl^-, but two different spectra are obtained after reduction by one electron under these two solution conditions. In the absence of added Cl^-, the one-electron reduced form of $Ru_2(2\text{-}CH_3ap)_4Cl$ exhibits a single absorption peak at 534 nm, but when excess Cl^- ion is present in solution the spectrum is characterized by three absorption bands at 450, 529, and 717 nm. The spectral data (as well as the electrochemical data to be discussed later) suggest an equilibrium between two forms of Ru_2^{4+}, one of which is formulated as $Ru_2(L)_4$ in CH_2Cl_2, 0.2 M TBAP, and the other as $[Ru_2(L)_4Cl]^-$ in CH_2Cl_2 containing 0.2 M TBAP and added TBACl.

The Ru_2^{4+} forms of the 2-Fap and 2,4,6-F_3ap complexes are also different in PhCN and DMSO as compared to

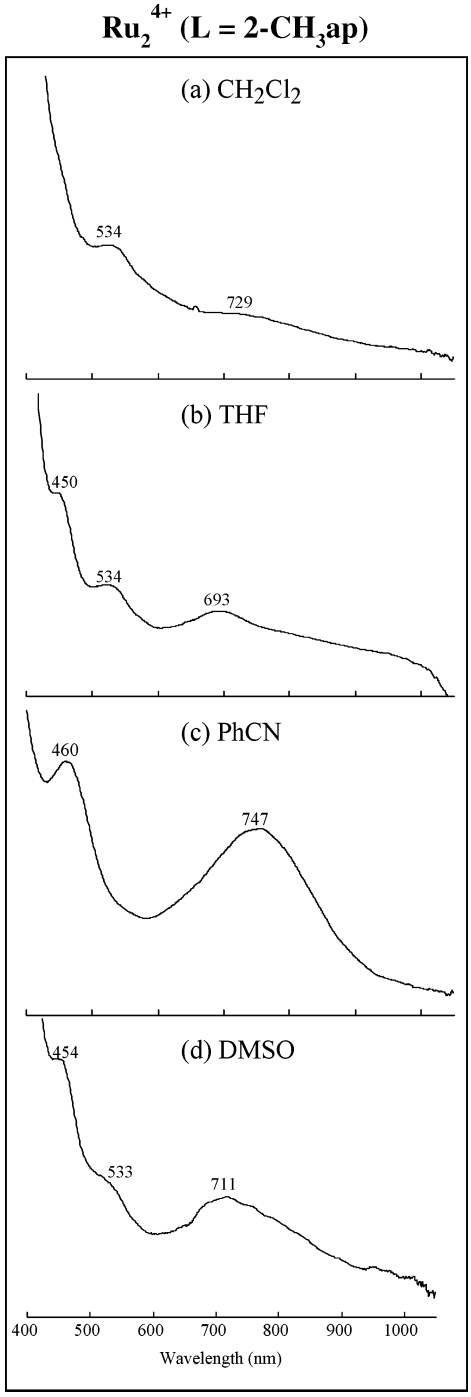

Figure 4. UV−vis spectra (400−1000 nm) (with arbitrary absorbance scale) of singly reduced $Ru_2(2\text{-}CH_3ap)_4Cl$ in (a) CH_2Cl_2, (b) THF, (c) PhCN, and (d) DMSO containing 0.2 M TBAP.

CH_2Cl_2 (see Table 3 and Figure S1), thus suggesting the formation of $Ru_2(L)_4(S)$ or $Ru_2(L)_4(S)_2$ (as opposed to $Ru_2(L)_4$) in the two coordinating solvents containing 0.1 M TBAP. The three Ru_2^{4+} complexes in PhCN (middle of Figure S1) are characterized by two sharp bands at 460−466 and 747−761 nm, and a similar pattern is also observed in DMSO where the three reduced compounds exhibit two bands at 452−486 and 711−782 nm (see bands labeled as I and IV in Table 3). This contrasts with what is observed in CH_2Cl_2 where the Ru_2^{4+} species have only a small shoulder peak at 476−534 nm (labeled as band II in Table 3) and no

(10) Bear, J. L.; Han, B.; Huang, S.; Kadish, K. M. *Inorg. Chem.* **1996**, *35*, 3012.
(11) Cotton, F. A.; Ren, T. *Inorg. Chem.* **1995**, *34*, 3190.

band close to 700 nm in the case of the compounds with L = 2-Fap or 2,4,6-F_3ap.

It should be noted that the Ru_2^{4+} form of $Ru_2(2\text{-}CH_3ap)_4Cl$ in DMSO and THF exhibits an absorption peak at 533−534 nm (band II) which is also seen in the optical spectrum of the same compound when it is reduced in CH_2Cl_2 (see Table 3). This result thus suggests three forms of the Ru_2^{4+} species depending upon the solvent. One of these forms is formulated as $Ru_2(L)_4$ (on the basis of the band at 533−534 nm) while the other two are formulated as $Ru_2(L)_4(S)_x$ ($x = 1$ or 2) in DMSO and $[Ru_2(L)_4Cl]^-$ in THF. The latter formulation is preferred over $Ru_2(L)(THF)_x$ (where $x = 1$ or 2) because THF ($\epsilon = 7.6$) is less polar than DMSO ($\epsilon = 46.4$) and the Cl^- ion is less likely to dissociate in THF.

Electrochemical Characterization of Ru_2^{4+}. The equilibrium between a solvent or Cl^- bound $Ru_2(L)_4$ in PhCN was electrochemically examined in the case of $Ru_2(2\text{-}CH_3ap)_4Cl$. As shown in Figure 1, reoxidation of the electrogenerated Ru_2^{4+} species in PhCN, 0.1 M TBAP, occurs via two processes that are located at $E_{pa} = -0.70$ V (peak 1a) and $E_{pa} = -0.36$ V (peak 1b). The more negative process is proposed to involve an oxidation of $[Ru_2(2\text{-}CH_3ap)_4Cl]^-$ while the peak at −0.36 V is attributed to an oxidation of $Ru_2(2\text{-}CH_3ap)_4(S)_x$ where $x = 1$ or 2.

In order to verify the above assignment, a PhCN solution of $Ru_2(2\text{-}CH_3ap)_4Cl$ containing 0.1 M TBAP was titrated with TBACl, and cyclic voltammograms were recorded after addition of each aliquot. Two reoxidations are seen after the initial reduction in PhCN, 0.1 M TBAP, but the peak assigned to the solvated species at $E_p = -0.36$ V disappears and only a single reversible reduction is obtained at $E_{1/2} = -0.81$ V in the presence of added TBACl. This is shown in Figure 6a and is consistent with the equilibrium shown in eq 4.

$$\underset{(E_{pa} = -0.70\ \text{V})}{[Ru_2^{4+}(L)_4Cl]^-} \underset{Cl}{\overset{S}{\rightleftharpoons}} \underset{(E_{pa} = -0.36\ \text{V})}{Ru_2^{4+}(L)_4(S)_x} \qquad (4)$$

The equilibrium in eq 4 could also be shifted toward the solvated form of Ru_2^{4+}, and these results are shown in Figure 6b which illustrates the change in electrochemical behavior as PhCN was added to a CH_2Cl_2 solution of $Ru_2(L)_4Cl$ containing 0.1 M TBAP. The process in CH_2Cl_2, 0.1 M TBAP, is reversible, but after the addition of 3 equiv of PhCN, a new process appears at $E_p = -0.40$ V as the major reoxidation peak which was originally at $E_{pa} = -0.89$ V decreases in intensity. Further addition of PhCN leads to further decreases in intensity of the peak at $E_p = -0.89$ V, and after the addition of 207 equiv of PhCN, the first reduction is totally irreversible as shown in the figure. These results are also consistent with the equilibrium shown in eq 4.

The current-voltage curves for electroreduction of $Ru_2(2\text{-}Fap)_4Cl$ and $Ru_2(2,4,6\text{-}F_3ap)_4Cl$ in PhCN containing 0.1 M TBAP resemble those of $Ru_2(2\text{-}CH_3ap)_4Cl$ under these same solution conditions (see Figure 1), thus suggesting that all three diruthenium compounds undergo a similar electron-transfer mechanism in PhCN.

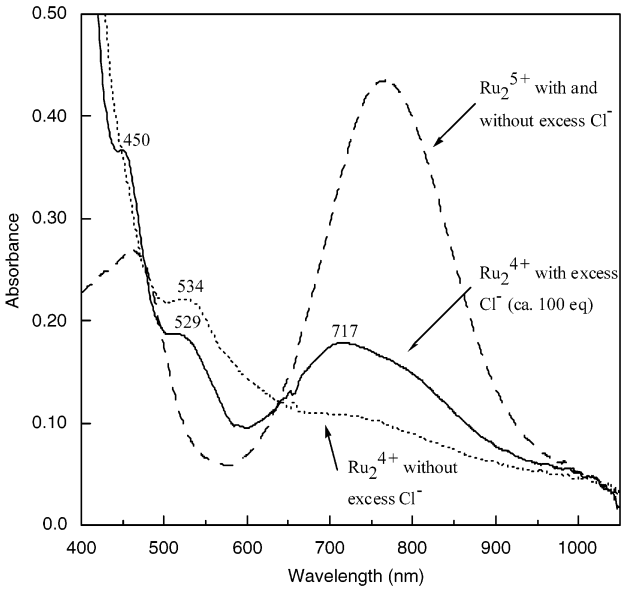

Figure 5. UV−vis specta of neutral (- - -) and singly reduced $Ru_2(2\text{-}CH_3ap)_4Cl$ in CH_2Cl_2 containg 0.2 M TBAP with (—) and without (•••) added TBACl in solution.

The exact number of solvent molecules bound to the Ru_2^{4+} species in the coordinating solvents was determined by measuring $E_{1/2}$ for reduction in CH_2Cl_2 containing increasing amounts of added solvent, either DMSO, PhCN, or DMF. Examples of two such plots of $E_{1/2}$ versus log[S] (S = DMF or PhCN) are given in Figure 7 for the case of $Ru_2(2\text{-}CH_3ap)_4Cl$ reduction in CH_2Cl_2 containing added DMF (Figure 7a) or PhCN (Figure 7b). The magnitude of the $\Delta E_{1/2}/\Delta\log[S]$ slopes agrees with the theoretically predicted 59 mV slope for the case where the reduced form of the compound has one more ligand than the neutral species,[12] thus suggesting that the Ru_2^{4+} form of $Ru_2(2\text{-}CH_3ap)_4$ should be formulated as $Ru_2(2\text{-}CH_3ap)_4(DMF)$ in neat DMF and $Ru_2(2\text{-}CH_3ap)_4(PhCN)$ in neat PhCN. Plots similar to those shown in Figure 7 were also obtained for the reduction of $Ru_2(2\text{-}CH_3ap)_4Cl$ in CH_2Cl_2 with added DMSO and the reduction of $Ru_2(2\text{-}Fap)_4Cl$ in CH_2Cl_2 with added DMF, DMSO, or PhCN, thus suggesting that the reduced forms of these two compounds can be formulated as $Ru_2(L)_4(S)$ where S = PhCN, DMF, and DMSO.

$Ru_2(2,4,6\text{-}F_3ap)_4Cl$ displays a different reductive behavior in the above three coordinating solvents. A plot of $E_{1/2}$ versus log[S] in CH_2Cl_2 containing added PhCN leads to a linear relationship and a 53 mV slope but in CH_2Cl_2/DMF or CH_2Cl_2/DMSO mixtures there is no shift at all in $E_{1/2}$ with increase in the DMF or DMSO concentration, thus indicating a lack of solvent binding to the Ru_2^{4+} complex under these solution conditions. It should be noted, however, that the UV−vis spectrum of singly reduced $Ru_2(2,4,6\text{-}F_3ap)_4Cl$ in neat DMSO (Figure S1) exhibits a pattern that can be accounted for by the binding of one solvent molecule to the Ru_2^{4+} form of the complex (see earlier discussion). This result is not inconsistent with the electrochemical data in CH_2Cl_2 containing added DMSO since under these conditions

(12) Kadish, K. M.; Bottomley, F.; Beroiz, D. *Inorg. Chem.* **1978**, *17*, 1124.

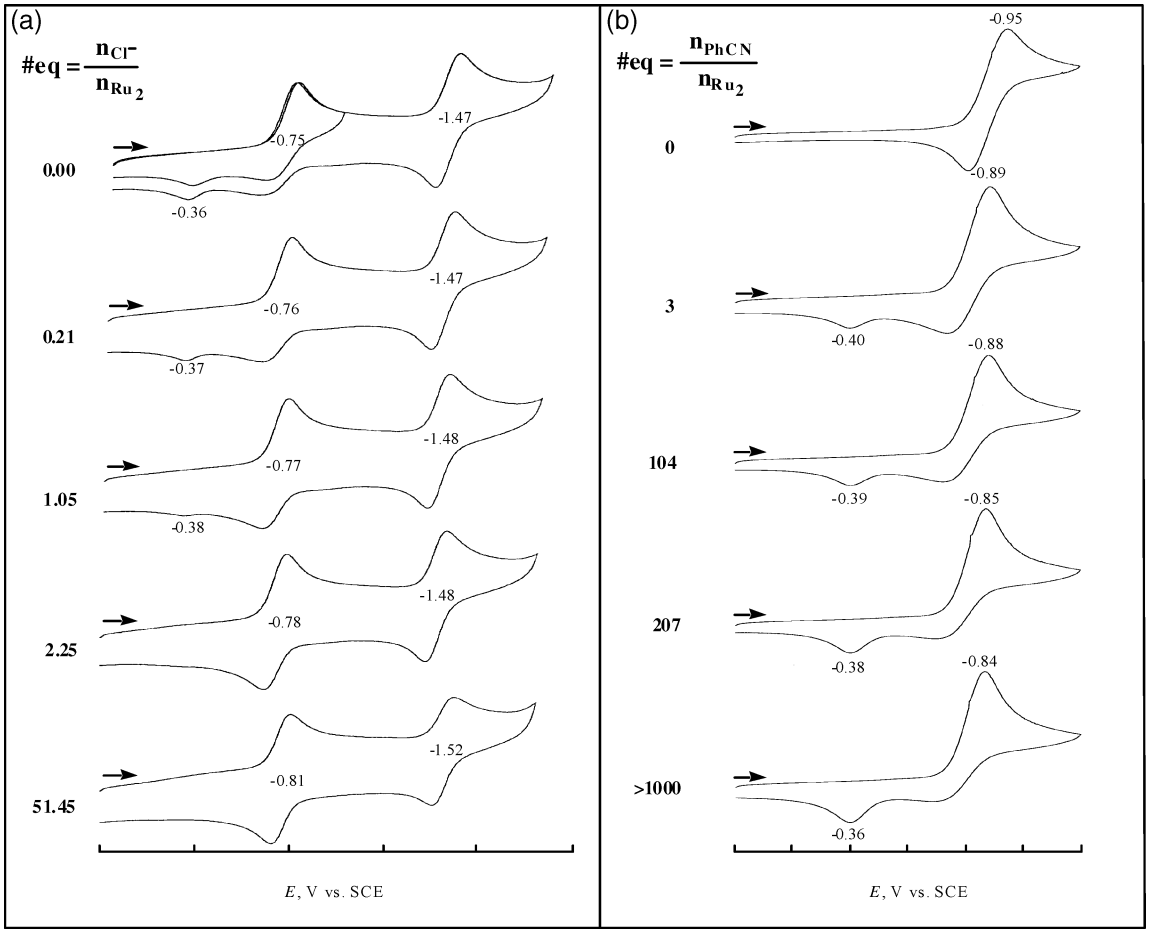

Figure 6. Cyclic voltammograms of $Ru_2(2\text{-}CH_3ap)_4Cl$ (a) in PhCN containing 0.1 M TBAP and increasing amounts of Cl^- and (b) in CH_2Cl_2 containing 0.1 M TBAP and increasing amounts of PhCN. Scan rate = 0.1 V/s.

the amount of DMSO in solution is much less than what is obtained in neat DMSO.

UV−Vis Characterization of Electrogenerated Ru_2^{6+}. UV−vis spectroelectrochemical experiments were also carried out during electrooxidation of each compound in CH_2Cl_2, PhCN, and DMSO in order to examine the Ru_2^{6+} absorption spectrum of each $Ru_2(L)_4Cl$ complex under these solution conditions. Figure 8 illustrates the UV−vis spectrum of each singly oxidized product in CH_2Cl_2, PhCN, and DMSO while a summary of the absorption peaks of each Ru_2^{6+} complex is given in Table 3. The spectroscopic data for singly oxidized $Ru_2(2\text{-}CH_3ap)_4Cl$ is consistent with the lack of solvent binding to the Ru_2^{6+} species, but differences in spectra do exist between the other two compounds upon going from S = CH_2Cl_2 to S = DMSO. This is especially evident in the case of $Ru_2(2\text{-}Fap)_4Cl$ where the major absorption band shifts from 960 to 780 nm. This result suggests a different degree of solvation to Ru_2^{6+} in CH_2Cl_2 and DMSO, and this point was further investigated utilizing electrochemical methods.

Electrochemical Characterization of Ru_2^{6+}. The oxidation of $Ru_2(L)_4Cl$ by one electron in the binding solvents PhCN, DMF, or DMSO will lead to compounds with a Ru_2^{6+} form which can, in principle, be formulated as $[Ru_2(L)_4Cl]^+$, $[Ru_2(L)_4Cl(S)]^+$, $[Ru_2(L)_4(S)]^{2+}$, or $[Ru_2(L)_4(S)_2]^{2+}$ depending upon the solvent. The number of solvent molecules axially coordinated to the Ru_2^{6+} species and the fate of the Cl^- ion upon oxidation were determined by examining the electrochemistry of each compound in mixed solvents as was done in the case of the first reduction (see Figure 7).

Figure 9a illustrates a plot of $E_{1/2}$ versus log[S] for the oxidation of $Ru_2(2\text{-}CH_3ap)_4Cl$ in CH_2Cl_2 containing added DMF while Figure 9b displays a similar type of plot for the oxidation of $Ru_2(2\text{-}Fap)_4Cl$ in CH_2Cl_2 with added DMSO. As seen in the figure, there is virtually no dependence of $E_{1/2}$ on the DMF concentration (the slope of 4 mV per 10-fold increase in [DMF] is simply attributed to junction potential differences upon addition of DMF to the CH_2Cl_2 solution), and this result is consistent with a lack of solvent coordination to singly oxidized $Ru_2(2\text{-}CH_3ap)_4Cl$. A similar conclusion (lack of solvent dependence on $E_{1/2}$) was also seen for oxidation of $Ru_2(2\text{-}CH_3ap)_4Cl$ in PhCN or DMSO and $Ru_2(2\text{-}Fap)_4Cl$ or $Ru_2(2,4,6\text{-}F_3ap)_4Cl$ in PhCN.

In contrast to these results, a Nernstian slope of −60 mV is obtained from $E_{1/2}$ versus log[DMSO] plots in CH_2Cl_2 containing DMSO at concentrations ranging from 0.1 to 3.2 M (Figure 9b), and this indicates that one DMSO molecule binds to the oxidized form of $Ru_2(2\text{-}Fap)_4Cl$ under these experimental conditions. A similar assignment can also be made for oxidation of $Ru_2(2\text{-}Fap)_4Cl$ in CH_2Cl_2/DMF mixtures where the Nernstian portion of the $E_{1/2}$ versus log[S] plot has a slope of −58 mV (Figure S2) and for oxidation

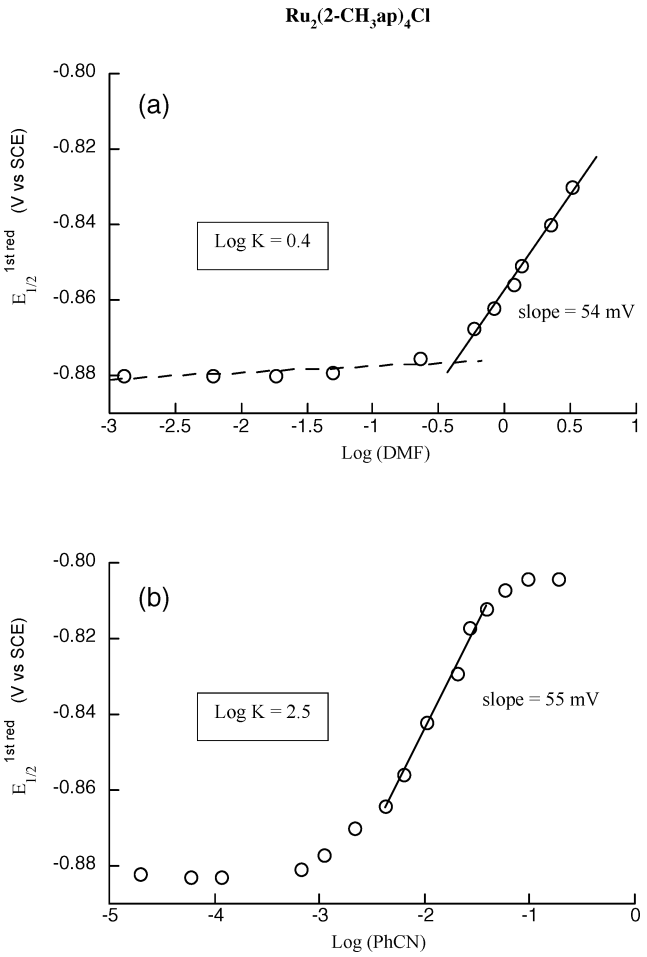

Figure 7. Plots of $E_{1/2}$ vs log[S] (S = DMF or PhCN) for reduction of $Ru_2(2\text{-}CH_3ap)_4Cl$ in CH_2Cl_2 containing 0.1 M TBAP and added (a) DMF or (b) PhCN.

of $Ru_2(2,4,6\text{-}F_3ap)_4Cl$ in CH_2Cl_2/DMF or CH_2Cl_2/DMSO mixtures where the $\Delta E_{1/2}/\Delta\log[S]$ slopes are −57 and −61 mV, respectively (Figure S3).

The Ru_2^{6+} form of $Ru_2(L)_4Cl$ (L = 2-Fap or 2,4,6-F_3ap) in neat DMF and DMSO can therefore be formulated as $[Ru_2(L)_4Cl(S)]^+$ if the solvent binds trans to the Cl^- ion or as $[Ru_2(L)_4(S)]^{2+}$ if the chloride ion is displaced by a solvent molecule after oxidation. In the first case, the σ-donor properties of a bound DMF or DMSO molecule will destabilize the HOMO, and the compound will be easier to oxidize in CH_2Cl_2/DMSO or CH_2Cl_2/DMF mixtures than in neat CH_2Cl_2. This is indeed what is observed as shown by the fact that the $\Delta E_{1/2}/\Delta\log[S]$ slopes are negative in all cases. Interestingly, the $Ru_2^{6+/5+}$ process of $Ru_2(2\text{-}Fap)_4Cl$ is characterized by two sets of peaks in neat DMSO or neat DMF (labeled as processes 3′ and 3″ in Figure 1), and the sum of the peak current intensity of these processes is about equal to that of process 1. This result can suggest that the neutral compound exists in two different forms in these solvents, i.e., $Ru_2(L)_4Cl$ and $Ru_2(L)_4Cl(S)$ (as was suggested earlier in the manuscript), or alternatively that $Ru_2(2\text{-}Fap)_4Cl$ is oxidized to $[Ru_2(2\text{-}Fap)_4Cl(S)]^+$ via process 3′ and to $[Ru_2(2\text{-}Fap)_4(S)]^{2+}$ or $[Ru_2(2\text{-}Fap)_4(S)_2]^{2+}$ via process 3″. The +2 charge on $[Ru_2(2\text{-}Fap)_4(S)_x]^{2+}$ (x = 1 or 2) would make the non-chloride bound form of the Ru_2^{6+} species more difficult to access than $[Ru_2(2\text{-}Fap)_4Cl(S)]^+$ or $[Ru_2(2\text{-}Fap)_4Cl]^+$, and consequently, process 3″ would occur at a more positive potential than either process 3 or process 3′. This is indeed what is seen from the potentials in Table 2.

Solvent Binding Constants to Ru_2^{4+} and Ru_2^{6+}. The data from $E_{1/2}$ versus log(S) plots of the type shown in Figures 7 and 9 were used to calculate binding constants for axial ligation to the Ru_2^{4+} and Ru_2^{6+} forms of the compounds using standard equations,[12] and data obtained for the three compounds in several coordinating solvents are given in Table 4. As seen from this table, PhCN does not bind to the Ru_2^{6+} form of any investigated compound, but this solvent possesses the largest binding constants for solvent coordination to the Ru_2^{4+} form of $Ru_2(L)_4Cl$ where L = 2-CH_3ap, 2-Fap, or 2,4,6-F_3ap. In addition, the binding properties of the singly reduced and singly oxidized forms of $Ru_2(L)_4Cl$ vary among the three derivatives. For example, $Ru_2(2\text{-}Fap)_4Cl$ exhibits the largest formation constant for solvent coordination to the Ru_2^{4+} species in all three binding solvents while the Ru_2^{6+} form of $Ru_2(2\text{-}CH_3ap)_4Cl$ has no affinity for DMF or DMSO as compared to the Ru_2^{6+} form of $Ru_2(2\text{-}Fap)_4Cl$ or $Ru_2(2,4,6\text{-}F_3ap)_4Cl$ under the same solution conditions.

In summary, the axial coordination of a solvent molecule to the Ru_2^{4+} or Ru_2^{6+} form of $Ru_2(L)_4Cl$ should involve an interaction between the HOMO and/or LUMO of the solvent and the π^* or σ^* orbitals of the dimetal complex as was shown upon axial coordination of pyrazine to $Ru_2(O_2CH)_4$.[13] The present study shows that the Ru_2^{6+} form of $Ru_2(2\text{-}CH_3ap)_4Cl$ differs from that of $Ru_2(2\text{-}Fap)_4Cl$ and $Ru_2(2,4,6\text{-}F_3ap)_4Cl$ in terms of its solvent binding ability, and this may be related to the different basicities of the three complexes since the 2-CH_3ap derivative ($\sum\sigma = -0.17$)[1] is more basic than either $Ru_2(2\text{-}Fap)_4Cl$ ($\sum\sigma = +0.24$)[1] or $Ru_2(2,4,6\text{-}F_3ap)_4Cl$ ($\sum\sigma = +0.54$).[1] Alternatively, the difference in solvent binding ability may be related to the isomer type since the 2-CH_3ap complex exists in a (4,0) conformation while the other two compounds exist in (3,1) conformations.[1]

Electronic Structure. The UV−vis spectrum of $Ru_2(L)_4Cl$ where L is a substituted ap ligand is characterized essentially by two intense features of similar molar absorptivity, one of which is usually split into two bands at 410−430 and 460−480 nm and the other consists of a single band which ranges from 750 to 950 nm.[1] We have recently shown that the exact position of the 750−950 nm band depends on the type of ligand and its mode of binding symmetry, i.e., (3,1) or (4,0) around the dimetal unit.[1] These two principal features of the spectrum have been assigned as π(Ru−N, Ru_2) → $\pi^*(Ru_2)$ or $\delta^*(Ru_2)$ where the significant amount of LMCT character has been accounted for by the fact that in an ap-type ligand the π(N) orbital is expected to be located at exceptionally high energy.[14] The spectrum of $Ru_2(L)_4Cl$ may in some cases also exhibit a weak absorption band at about 600 nm,[1] and possible metal−metal transitions of the

(13) Wesemann, J. L.; Chisholm, M. H. *Inorg. Chem.* **1997**, *36*, 3258.
(14) Miskowski, V. M.; Hopkins, M. D.; Winkler, J. R.; Gray, H. B. Multiple Metal−Metal Bonds. In *Inorganic Electronic Structure and Spectroscopy*; Solomon, E. I., Lever, A. B. P., Eds.; Vol. II, p 343.

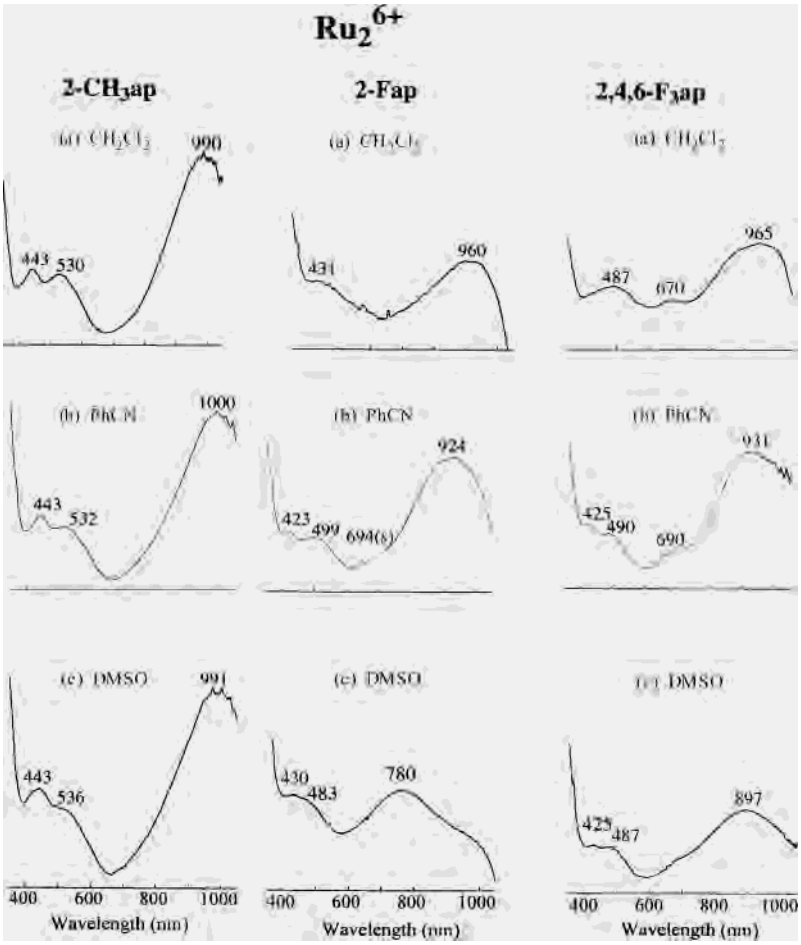

Figure 8. UV−vis spectra (400−1000 nm) (with arbitrary absorbance scale) of singly oxidized $Ru_2(L)_4Cl$ where L = 2-CH_3ap, 2-Fap, or 2,4,6-F_3ap in (a) CH_2Cl_2, (b) PhCN, and (c) DMSO containing 0.2 M TBAP.

type $\delta \rightarrow \pi^*$, $\delta^* \rightarrow \sigma^*$, $\pi^* \rightarrow \sigma^*$ have been proposed for this transition.[14,15]

$Ru_2(L)_4Cl$ where L = 2-CH_3ap, 2-Fap, or 2,4,6-F_3ap exhibits a room-temperature magnetic moment in CD_2Cl_2 which ranges from 3.84 to 3.95 μ_B,[1,8] and these values can be compared to magnetic moments of 3.77 μ_B for Ru_2(2-CH_3ap)$_4$Cl and Ru_2(2-Fap)$_4$Cl and 3.93 for Ru_2(2,4,6-F_3ap)$_4$Cl in DMSO-d_6, thus indicating the presence of 3 unpaired electrons which is consistent with the same electronic configuration of $\sigma^2\pi^4\delta^2\pi^{*2}\delta^*$ for the three compounds, independent of the solvent polarity. This conclusion also agrees with the UV−vis data of the neutral Ru_2^{5+} complexes which show no evidence for displacement of the Cl^- ion by any of the five investigated solvents and therefore should have the same formulation, i.e., $Ru_2(L)_4Cl$ in all cases.

The electronic configuration of several reduced compounds of the type $Ru_2(L)_4Cl$ in their neutral form (where L is a substituted ap ligand) has been proposed as $\sigma^2\pi^4\delta^2\pi^{*3}\delta^*$ on the basis of electrochemical substituent effects.[1] Such an assignment is consistent with the presence of two unpaired electrons, and this is indeed the case as indicated by the fact that singly reduced Ru_2(2-Fap)$_4$Cl and Ru_2(2,4,6-F_3ap)$_4$Cl possess magnetic moments of 2.70 and 2.79 μ_B, respectively, in CD_2Cl_2 at room temperature. The electronic configuration $\sigma^2\pi^4\delta^2\pi^{*3}\delta^*$ also agrees with the UV−vis spectrum of the singly reduced compounds in CH_2Cl_2 which lacks most of the features associated with transitions of the type π(Ru−N, Ru_2) $\rightarrow \pi^*$(Ru_2) or δ^*(Ru_2). This result is expected if the additional electron is added to the π^* orbital and if the transition involves the π^* and not the δ^* orbital.

Interestingly, the UV−vis spectrum of the Ru_2^{4+} species in PhCN exhibits features which differ significantly from those seen in CH_2Cl_2, but it also somewhat parallels what is seen for the Ru_2^{5+} complex in the same solvent (see Table 3) because in both cases there are two main absorption bands having similar molar absorptivities. Since the electrochemical titration clearly indicates that one molecule of PhCN axially binds to singly reduced $Ru_2(L)_4Cl$ in a CH_2Cl_2/PhCN mixture, one likely possibility is that axial coordination of PhCN to the Ru_2^{4+} form of the compound switches the electronic configuration from $\sigma^2\pi^4\delta^2\pi^{*3}\delta^*$ to $\sigma^2\pi^4\delta^2\pi^{*2}\delta^{*2}$. Unfortunately, one cannot distinguish between these two electronic configurations on the basis of room-temperature magnetic data alone, and we were not able to confirm this assumption by isolating the reduced products in their solid state in order to determine the magnetic moment of the compounds over a large range of temperatures.

The electronic configuration for the singly oxidized Ru_2^{6+} form of $Ru_2(ap)_4Cl$ was proposed[16] as $\sigma^2\pi^4\delta^2\pi^{*2}$. The same

(15) Miskowski, V. M.; Gray, H. B. *Inorg. Chem.* **1988**, *27*, 2501.

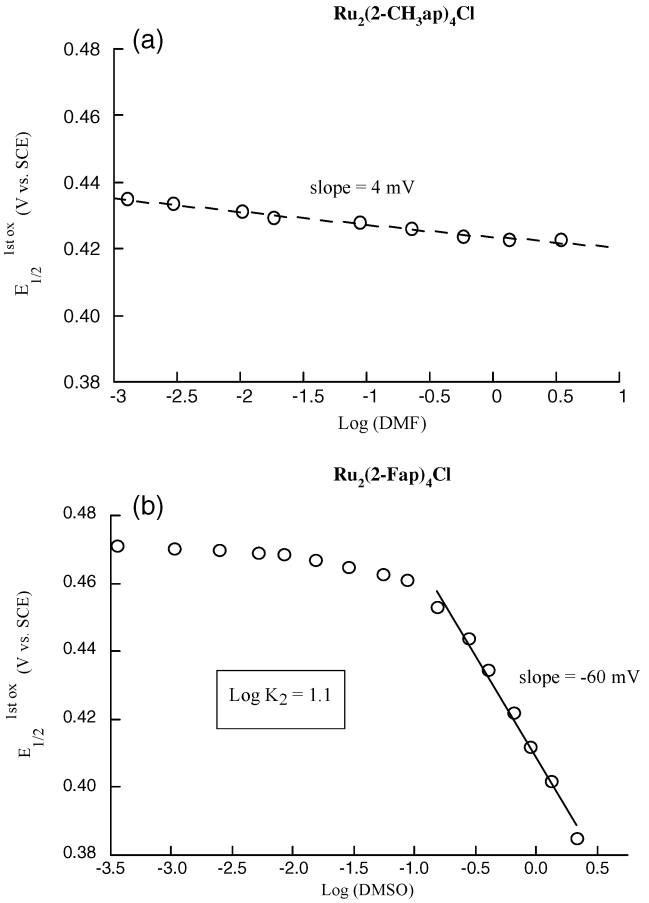

Figure 9. Plots of $E_{1/2}$ vs log[S] (S = DMF or DMSO) for oxidation of (a) $Ru_2(2\text{-}CH_3ap)_4Cl$ in CH_2Cl_2 containing 0.1 M TBAP and added DMF and (b) $Ru_2(2\text{-}Fap)_4Cl$ in CH_2Cl_2 containing 0.1 M TBAP and added DMSO.

electronic configuration has recently been suggested for each oxidized form of $Ru_2(L)_4Cl$ (L is a substituted ap ligand) in CH_2Cl_2 since in this solvent all compounds exhibit virtually the same UV−vis spectra, independent of the bridging ligand.[1] The room-temperature magnetic moments of singly oxidized $Ru_2(2\text{-}Fap)_4Cl$ and $Ru_2(2,4,6\text{-}F_3ap)_4Cl$ in CD_2Cl_2 are 2.65 and 2.53 μ_B, respectively. These values are close to the 2.75−2.90 μ_B range for other Ru_2^{6+} complexes whose electronic ground states have been proposed to agree with the presence of two unpaired electrons[14] and are thus consistent with the suggested electronic configuration $\sigma^2\pi^4\delta^2\pi^{*2}$.

Table 4. Binding Constants for the Axial Ligation of Solvent to the Ru_2^{4+} and Ru_2^{6+} Oxidation States of Investigated $Ru_2(L)_4Cl$ Complexes

	binding constant (log *K*)					
	$Ru_2^{4+}(L)_4 + S \rightleftharpoons Ru_2^{4+}(L)_4(S)$			$[Ru_2^{6+}(L)_4Cl]^+ + S \rightleftharpoons [Ru_2^{6+}(L)_4Cl(S)]^+$		
solvent	2-CH_3ap	2-Fap	2,4,6-F_3ap	2-CH_3ap	2-Fap	2,4,6-F_3ap
PhCN	2.5	4.0	0.9	no rxn	no rxn	no rxn
DMF	0.4	1.6	no rxn[a]	no rxn	1.4	1.3
DMSO	0.8	1.2	no rxn[a]	no rxn	1.1	1.3

[a] On the basis of electrochemical data in mixed solvent systems.

Since the electrochemical data in CH_2Cl_2/PhCN mixtures indicate that there is no coordination of solvent to the oxidized forms of $Ru_2(L)_4Cl$ where L = 2-CH_3ap, 2-Fap, or 2,4,6-F_3ap, the same $\sigma^2\pi^4\delta^2\pi^{*2}$ electronic configuration can be proposed for the Ru_2^{6+} species in CH_2Cl_2 and PhCN (or CD_3CN) as well as in all of the solvents that do not bind to the Ru_2^{6+} form of the compounds (see Table 4).

Although there are obvious differences in the positions of the spectral absorption bands of oxidized $Ru_2(L)_4Cl$ (L = 2-Fap or 2,4,6-F_3ap) in CH_2Cl_2, DMF, or DMSO (the electrochemical data indicates a coordination of one solvent molecule upon oxidation in CH_2Cl_2/DMF and CH_2Cl_2/DMSO mixtures), the overall shape of the UV−vis spectrum does not change significantly upon going from one solvent to another, thus suggesting no changes of the electronic ground state upon coordination of DMSO to the Ru_2^{6+} complexes. The room-temperature magnetic moment of $[Ru_2(2\text{-}Fap)_4Cl]^+$ in DMSO-d_6 was measured as 3.03 μ_B, and this value is also consistent with the electronic ground state $\sigma^2\pi^4\delta^2\pi^{*2}$.

Acknowledgment. The support of the Robert A. Welch Foundation (J.L.B., Grant E-918; K.M.K., Grant E-680) is gratefully acknowledged. E.V.C. and R.G. also thank the Robert A. Welch Foundation for their HBU departmental grant (Grant BF-0016).

Supporting Information Available: Figures for the UV−vis spectra of the reduced forms of the compounds as well as plots of $E_{1/2}$ vs log(S) (S is DMF or DMSO) for reduction and oxidation of $Ru_2(2\text{-}Fap)_4Cl$ and $Ru_2(2,4,6\text{-}F_3ap)_4Cl$. This material is available free of charge via the Internet at http://pubs.acs.org.

IC034722D

(16) Cotton, F. A.; Yokochi, A. *Inorg. Chem.* **1997**, *36*, 567.